Direct Observation of the Dynamic Process Underlying Allosteric Signal Transmission

ARTICLE *in* JOURNAL OF THE AMERICAN CHEMICAL SOCIETY · MARCH 2009

Impact Factor: 12.11 · DOI: 10.1021/ja809947w · Source: PubMed

7 AUTHORS, INCLUDING:

Paul Schanda
Institut de Biologie Structurale (IBS)
50 PUBLICATIONS **1,733** CITATIONS
SEE PROFILE

Georg Kontaxis
University of Vienna
46 PUBLICATIONS **1,470** CITATIONS
SEE PROFILE

Robert Konrat
University of Vienna
134 PUBLICATIONS **2,901** CITATIONS
SEE PROFILE

Martin Tollinger
University of Vienna
38 PUBLICATIONS **1,033** CITATIONS
SEE PROFILE

J|A|C|S ARTICLES

Published on Web 02/09/2009

Direct Observation of the Dynamic Process Underlying Allosteric Signal Transmission

Sven Brüschweiler,[†] Paul Schanda,[‡,§] Karin Kloiber,[†] Bernhard Brutscher,[‡] Georg Kontaxis,[†] Robert Konrat,[†] and Martin Tollinger*[,†]

Department of Computational & Structural Biology, Max F. Perutz Laboratories, Campus Vienna Biocenter 5, A-1030 Vienna, Austria and Institut de Biologie Structurale Jean-Pierre Ebel, CNRS, CEA, UJF, 41 rue Jules Horowitz, F-38027 Grenoble, France

Received December 20, 2008; E-mail: martin.tollinger@univie.ac.at

Abstract: Allosteric regulation is an effective mechanism of control in biological processes. In allosteric proteins a signal originating at one site in the molecule is communicated through the protein structure to trigger a specific response at a remote site. Using NMR relaxation dispersion techniques we directly observe the dynamic process through which the KIX domain of CREB binding protein communicates allosteric information between binding sites. KIX mediates cooperativity between pairs of transcription factors through binding to two distinct interaction surfaces in an allosteric manner. We show that binding the activation domain of the mixed lineage leukemia (MLL) transcription factor to KIX induces a redistribution of the relative populations of KIX conformations toward a high-energy state in which the allosterically activated second binding site is already preformed, consistent with the Monod−Wyman−Changeux (WMC) model of allostery. The structural rearrangement process that links the two conformers and by which allosteric information is communicated occurs with a time constant of 3 ms at 27 °C. Our dynamic NMR data reveal that an evolutionarily conserved network of hydrophobic amino acids constitutes the pathway through which information is transmitted.

Introduction

Allostery requires that information about the presence (or absence) of a biological target can be communicated between remote sites of protein molecules. While allosteric regulation plays a key role in many biological events on a molecular level,[1] the exact biophysical characterization of the mechanisms by which allosteric communication occurs remains a major challenge in structural biology.[2−4] Traditionally, allosteric mechanisms have been investigated by comparing static three-dimensional structures of proteins in their limiting states, i.e., the structures of unliganded beginning and ligand-bound end states.[5] Allosteric communication is, however, intimately linked to protein dynamics[6−11] and can be characterized at atomic resolution by NMR spin relaxation techniques.[12] With the exception of purely dynamics-driven allostery,[13] allosteric information is typically transmitted by means of conformational changes along a defined pathway.[14] To characterize conformational transitions in proteins, NMR relaxation dispersion techniques can be employed. These experiments allow the quantitative study of transitions between states even in cases with highly skewed populations where low-populated (minor) states are not directly observable and allow extracting information about the time-scale of the transition as well as the structures of these low-populated states in terms of chemical shifts and residual anisotropic interactions.[15,16]

Here, we characterize the molecular mechanism through which the KIX domain of CREB-binding protein, CBP, propagates allosteric information between two remote binding sites. CBP is a transcriptional coactivator that is involved in a variety of biological processes such as cellular differentiation, development, and growth control.[17] CBP acts as a scaffold for the assembly of the transcriptional machinery through binding of transcription factors, which in turn bind to DNA promoter sequences. Interactions with transcription factors are mediated by independently folded protein modules; one such modular

[†] Max F. Perutz Laboratories.
[‡] Institut de Biologie Structurale Jean-Pierre Ebel.
[§] Current address: Physical Chemistry, ETH Zürich, Wolfgang-Pauli Strasse 10, CH-8093 Zürich, Switzerland.

(1) Hardy, J. A.; Wells, J. A. *Curr. Opin. Struct. Biol.* **2004**, *14*, 706–715.
(2) Goodey, N. M.; Benkovic, S. J. *Nat. Chem. Biol.* **2008**, *4*, 474–482.
(3) Cui, Q.; Karplus, M. *Protein Sci.* **2008**, *17*, 1295–1307.
(4) Kumar, S.; Ma, B.; Tsai, C. J.; Sinha, N.; Nussinov, R. *Protein Sci.* **2000**, *9*, 10–19.
(5) Daily, M. D.; Gray, J. J. *Proteins* **2007**, *67*, 385–399.
(6) Swain, J. F.; Gierasch, L. M. *Curr. Opin. Struct. Biol.* **2006**, *16*, 102–108.
(7) Kern, D.; Zuiderweg, E. R. *Curr. Opin. Struct. Biol.* **2003**, *13*, 748–757.
(8) Volkman, B. F.; Lipson, D.; Wemmer, D. E.; Kern, D. *Science* **2001**, *291*, 2429–2433.
(9) Velyvis, A.; Yang, Y. R.; Schachman, H. K.; Kay, L. E. *Proc. Natl. Acad. Sci. U.S.A.* **2007**, *104*, 8815–8820.
(10) Popovych, N.; Sun, S.; Ebright, R. H.; Kalodimos, C. G. *Nat. Struct. Mol. Biol.* **2006**, *13*, 831–838.
(11) Gunasekaran, K.; Ma, B.; Nussinov, R. *Proteins* **2004**, *57*, 433–443.
(12) Mittermaier, A.; Kay, L. E. *Science* **2006**, *312*, 224–228.
(13) Cooper, A.; Dryden, D. T. *Eur. Biophys. J.* **1984**, *11*, 103–109.
(14) Tsai, C. J.; del Sol, A.; Nussinov, R. *J. Mol. Biol.* **2008**, *378*, 1–11.
(15) Hansen, D. F.; Vallurupalli, P.; Kay, L. E. *J. Biomol. NMR* **2008**, *41*, 113–120.
(16) Korzhnev, D. M.; Kay, L. E. *Acc. Chem. Res.* **2008**, *41*, 442–451.
(17) Goodman, R. H.; Smolik, S. *Genes Dev.* **2000**, *14*, 1553–1577.

protein-binding domain in CBP is KIX, a small single-domain protein whose fold is composed of a bundle of three α helices and two short 3_{10} helices (see Figure S1 in the Supporting Information).[18] The KIX domain interlinks a great variety of different transcription factors by simultaneous binding through two interaction sites. One of these sites binds, for example, the activation domain of the mixed lineage leukemia (MLL) protein,[19] whereas the activation domain of the transcription factor c-Myb (among others) binds to the remote second site on KIX.[20] In vitro, binding of the MLL activation domain to KIX cooperatively enhances the interaction with c-Myb through an unknown allosteric mechanism:[19] KIX in complex with MLL displays a ∼2-fold higher affinity for the c-Myb activation domain than the KIX domain alone.[21] Our dynamic NMR analysis of allosteric communication in KIX provides a quantitative description of the mechanism through which this domain mediates cooperativity between transcription factors.

Materials and Methods

Sample Preparation. Samples of uniformly ^{13}C- and/or ^{15}N-labeled KIX (residues 586−672) were prepared by bacterial growth using standard procedures and purified as described.[22] Selective ^{13}C labeling at backbone C^{α} and isoleucine side chain $C^{\delta 1}$ positions was obtained by supplementing growth media with 2-^{13}C-glucose[23] and 4-^{13}C-α-ketobutyrate,[24,25] respectively. Peptides that include the minimal activation domains of transcription factors, corresponding to residues 2840−2858 of MLL[19] (with Ala substituting for Cys2841),[21] residues 291−315 of c-Myb,[26] and residues 116−149 of CREB (with Ser-133 phosphorylated),[27] were purchased from PSL (Heidelberg, Germany).

NMR Spectroscopy and Data Analysis. NMR samples contained 0.4−1.0 mM KIX, 50 mM potassium phosphate buffer, pH 5.8, 25 mM NaCl, and 1 mM NaN_3 in 8% D_2O/92% H_2O. ^{15}N, $^{13}C^{\alpha}$, and $^{13}C^{\delta 1}$ Carr−Purcell−Meiboom−Gill (CPMG) relaxation dispersion experiments were performed at ^1H Larmor frequencies of 500, 600, and 800 MHz and 27 °C as described,[28−30] yielding data for 73 ^{15}N, 42 $^{13}C^{\alpha}$, and 3 Ile-$^{13}C^{\delta 1}$ sites. All dispersion profiles were numerically fitted to a common two-state process (assuming a more complicated kinetic scheme by inclusion of a third state into the model did not lead to a statistically significant improvement of the fit, as judged by *F*-test criteria).[31] For Tyr648 (^{15}N) the data could not be fitted by a common process, and this residue was excluded from further analysis. In the first step of the fitting procedure, data from residues with exchange contributions exceeding 3 s^{-1} at 800 MHz (18 residues) were employed to determine the time-scale of the exchange process, τ_{ex}, and the populations of states, p_i (assuming identical values of τ_{ex} and p_i for all nuclei but residue-specific values for $\Delta\omega$). Data for residues with exchange contributions < 3 s^{-1} were subsequently fitted individually with τ_{ex} and p_i constrained to the values obtained by this procedure to determine their $\Delta\omega_{disp}$ values. Uncertainties were estimated via a Monte Carlo approach using 1000 synthetic data sets generated on the basis of repeat experiments, and standard deviations are reported in all cases. Backbone amide H/D exchange rates were measured using the SOFAST real-time approach and compared to the exchange rates of unprotected amide hydrogens as described.[32]

Results and Discussion

Figure 1a shows experimental relaxation dispersion data obtained for backbone amide ^{15}N and $^{13}C^{\alpha}$ nuclei in the binary complex formed by KIX and the activation domain of MLL. Nonflat relaxation dispersion profiles are detected for most residues in KIX·MLL, suggesting the presence of a conformational transition on the micro- to millisecond time-scale. Analysis of the data shows that this process occurs with a time constant of 3.0 ± 0.3 ms at 27 °C between two states that are populated to 93.0 ± 0.3% and 7.0 ± 0.3%, respectively. Dispersion profiles for all nuclei can be consistently fitted to the same dynamic parameters, indicative of a collective nature of the underlying conformational transition. All observed ^{15}N and $^{13}C^{\alpha}$ chemical shift differences between the two conformers, $\Delta\omega_{disp}$, are small (Figure 1b). Protein NMR chemical shifts are sensitive reporters of local structure;[33] the small magnitude of the $\Delta\omega_{disp}$ values suggests that the two states differ only marginally in their backbone conformation, ruling out (local) unfolding as an underlying process. Rather, the ^{15}N and $^{13}C^{\alpha}$ data imply that the minor (7%) state represents an alternative, folded conformer. Consistently, backbone amide hydrogen/deuterium exchange data on the KIX·MLL complex show that both states represent solvent exchange protected and fully folded conformers (Figure S2 in the Supporting Information), and temperature-dependent relaxation dispersion data show that the equilibrium between these conformers is almost invariant with temperature, indicating that the two states are of similar enthalpy (Figure S3 in the Supporting Information). Notably, the relaxation dispersion $\Delta\omega_{disp}$ values ($^{15}N/^{13}C^{\alpha}$) exceed 0.5 ppm only for residues close to the carboxy-terminal region of helix α_1 as well as residues in the center of helix α_3, encompassing parts of the MLL and c-Myb binding sites, respectively.

While the minor population is not directly observable in NMR spectra, the conformational transition between the two states gives rise to population-weighted resonance positions. Upon addition of the c-Myb activation domain to the binary KIX·MLL complex, KIX resonances gradually approach the chemical shifts of the ternary KIX·MLL·c-Myb complex (Figure 2a). The absolute values of the ^{15}N chemical shift differences that we measure between the ternary and the binary complex, $\Delta\omega_{ternary\text{-}binary}$, clearly correlate with the chemical shift differences between major and minor populations of the binary complex determined by relaxation

(18) De Guzman, R. N.; Goto, N. K.; Dyson, H. J.; Wright, P. E. *J. Mol. Biol.* **2006**, *355*, 1005–1013.
(19) Ernst, P.; Wang, J.; Huang, M.; Goodman, R. H.; Korsmeyer, S. J. *Mol. Cell. Biol.* **2001**, *21*, 2249–2258.
(20) Parker, D.; Rivera, M.; Zor, T.; Henrion-Caude, A.; Radhakrishnan, I.; Kumar, A.; Shapiro, L. H.; Wright, P. E.; Montminy, M.; Brindle, P. K. *Mol. Cell. Biol.* **1999**, *19*, 5601–5607.
(21) Goto, N. K.; Zor, T.; Martinez-Yamout, M.; Dyson, H. J.; Wright, P. E. *J. Biol. Chem.* **2002**, *277*, 43168–43174.
(22) Rutledge, S. E.; Volkman, H. M.; Schepartz, A. *J. Am. Chem. Soc.* **2003**, *125*, 14336–14347.
(23) Lundström, P.; Teilum, K.; Carstensen, T.; Bezsonova, I.; Wiesner, S.; Hansen, D. F.; Religa, T. L.; Akke, M.; Kay, L. E. *J. Biomol. NMR* **2007**, *38*, 199–212.
(24) Goto, N. K.; Gardner, K. H.; Mueller, G. A.; Willis, R. C.; Kay, L. E. *J. Biomol. NMR* **1999**, *13*, 369–374.
(25) Lichtenecker, R.; Ludwiczek, M. L.; Schmid, W.; Konrat, R. *J. Am. Chem. Soc.* **2004**, *126*, 5348–5349.
(26) Parker, D.; Jhala, U. S.; Radhakrishnan, I.; Yaffe, M. B.; Reyes, C.; Shulman, A. I.; Cantley, L. C.; Wright, P. E.; Montminy, M. *Mol. Cell* **1998**, *2*, 353–359.
(27) Parker, D.; Ferreri, K.; Nakajima, T.; LaMorte, V. J.; Evans, R.; Koerber, S. C.; Hoeger, C.; Montminy, M. R. *Mol. Cell. Biol.* **1996**, *16*, 694–703.
(28) Tollinger, M.; Skrynnikov, N. R.; Mulder, F. A.; Forman-Kay, J. D.; Kay, L. E. *J. Am. Chem. Soc.* **2001**, *123*, 11341–11352.
(29) Hansen, D. F.; Vallurupalli, P.; Lundstrom, P.; Neudecker, P.; Kay, L. E. *J. Am. Chem. Soc.* **2008**, *130*, 2667–2675.
(30) Skrynnikov, N. R.; Mulder, F. A.; Hon, B.; Dahlquist, F. W.; Kay, L. E. *J. Am. Chem. Soc.* **2001**, *123*, 4556–4566.
(31) McConnell, H. M. *J. Chem. Phys.* **1958**, *28*, 430–431.
(32) Schanda, P.; Brutscher, B.; Konrat, R.; Tollinger, M. *J. Mol. Biol.* **2008**, *380*, 726–741.
(33) Shen, Y.; et al. *Proc. Natl. Acad. Sci. U.S.A.* **2008**, *105*, 4685–4690.

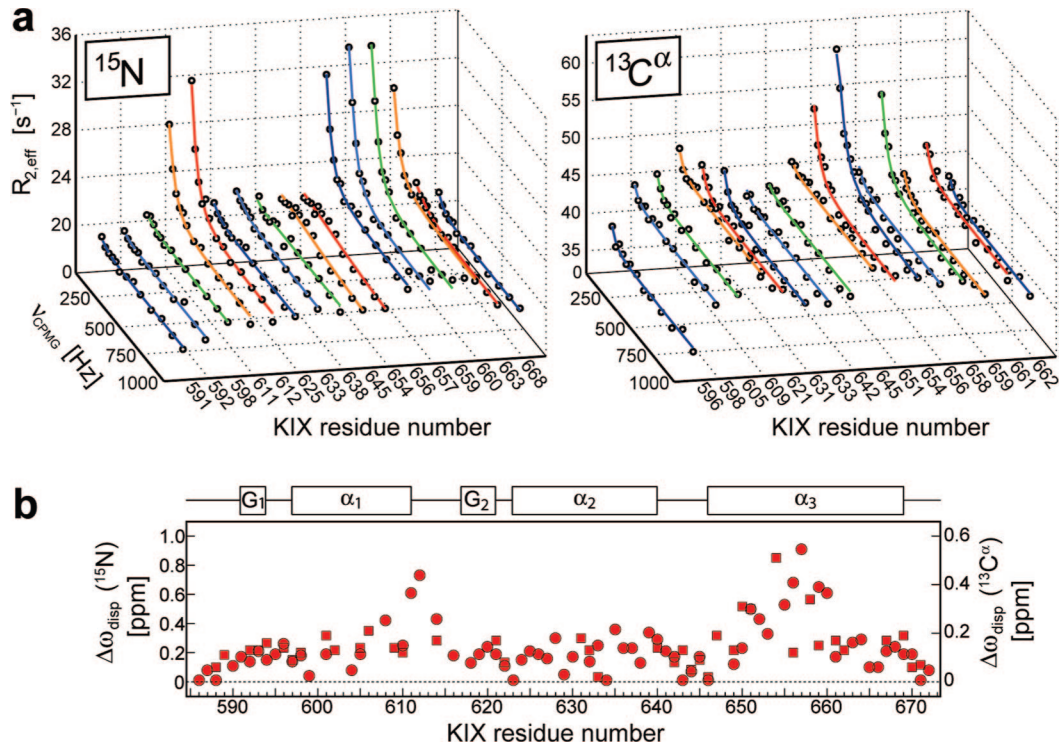

Figure 1. NMR relaxation dispersion data for the KIX·MLL complex. (a) ^{15}N (left) and $^{13}C^{\alpha}$ (right) relaxation dispersion profiles for representative residues of KIX bound to MLL (concentration ratio KIX:MLL = 1:2.2), recorded at 800 MHz and 27 °C, along with best fits (lines). Under these conditions, >99.7% of KIX molecules are bound to MLL (K_d = 2.8 μM).[21] (b) Absolute values of backbone ^{15}N (circles) and $^{13}C^{\alpha}$ (squares) chemical shift differences between the two KIX conformations, $\Delta\omega_{disp}$, as determined from the relaxation dispersion data for KIX·MLL. The location of the α helices and 3_{10} helices in KIX is indicated (PDB entry code 2AGH).[18]

dispersion measurements (Figure 2b). The linear correlation coefficient between the two data sets is 0.79 (Figure 2c), and a similar correlation is obtained for $^{13}C^{\alpha}$ nuclei (Figure S4 in the Supporting Information), demonstrating that the conformation of KIX in the minor state of binary KIX·MLL is similar to KIX in the ternary KIX·MLL·c-Myb complex. Moreover, these data suggest that chemical shift changes upon binding of c-Myb to KIX·MLL are governed by conformational changes of KIX in response to ligand binding rather than local effects caused by direct contacts with the ligand peptide. This is corroborated by the chemical shift changes that we observe upon ternary complex formation using an alternative ligand: binding of the phosphorylated kinase-inducible domain (pKID) of CREB to KIX·MLL results in very similar backbone ^{15}N and $^{13}C^{\alpha}$ chemical shift changes for the majority of KIX residues with the exception of residues that are involved in specific interactions with charged and/or aromatic pKID side chains that are absent in c-Myb (Figure S5).

It is of particlar interest to clarify whether the minor state of KIX that is populated to 7% in the binary KIX·MLL complex is populated prior to MLL binding. To address this question we performed backbone ^{15}N relaxation dispersion experiments at variable KIX:MLL concentration ratios, ranging between 1:0 and 1:2.2 (Figure 3). The data clearly show that the minor state of KIX is not populated to an appreciable degree (<~0.5%) in the absence of MLL but becomes progressively populated as the binary KIX·MLL complex is formed. This indicates that binding the activation domain of the MLL transcription factor to KIX induces a redistribution of the relative populations of KIX conformations toward a state in which the c-Myb (pKID) binding site is already preformed.

Because the conformation of KIX in the minor state of KIX·MLL already resembles the ternary complex, this state might be expected to display a higher affinity for c-Myb (or pKID).[34] This can be verified in a straightforward manner: As either c-Myb or pKID bind to KIX·MLL to form a ternary complex, the equilibrium between major and minor states will shift toward the state that binds ligand with higher affinity. The observation that ^{15}N and $^{13}C^{\alpha}$ $\Delta\omega_{ternary\text{-}binary}$ values are of similar magnitude as the relaxation dispersion $\Delta\omega_{disp}$ values (Figure 2c) implies that it is the minor state toward which the equilibrium shifts and therefore represents the higher affinity conformation. The interaction between KIX and ligands thus involves selection from a pre-existing ensemble of conformations.[35,36] In the presence of saturating amounts of ligands binding to both KIX interaction sites relaxation dispersion profiles are flat (Figure 4).

Taken together, our data unequivocally establish that in the binary KIX·MLL complex KIX spontaneously interconverts between a major (lower energy) state and a minor (higher energy) state, which adopts a conformation similar to that of the ternary complex and binds c-Myb with higher affinity. Such a mechanism is consistent with the WMC model of allostery, which implies that the conformational transition that mediates information transfer between binding sites involves states that

(34) Tsai, C. J.; Kumar, S.; Ma, B.; Nussinov, R. *Protein Sci.* **1999**, *8*, 1181–1190.
(35) Ma, B.; Kumar, S.; Tsai, C. J.; Nussinov, R. *Protein Eng.* **1999**, *12*, 713–720.
(36) Lange, O. F.; Lakomek, N. A.; Fares, C.; Schröder, G. F.; Walter, K. F.; Becker, S.; Meiler, J.; Grubmüller, H.; Griesinger, C.; de Groot, B. L. *Science* **2008**, *320*, 1471–1475.

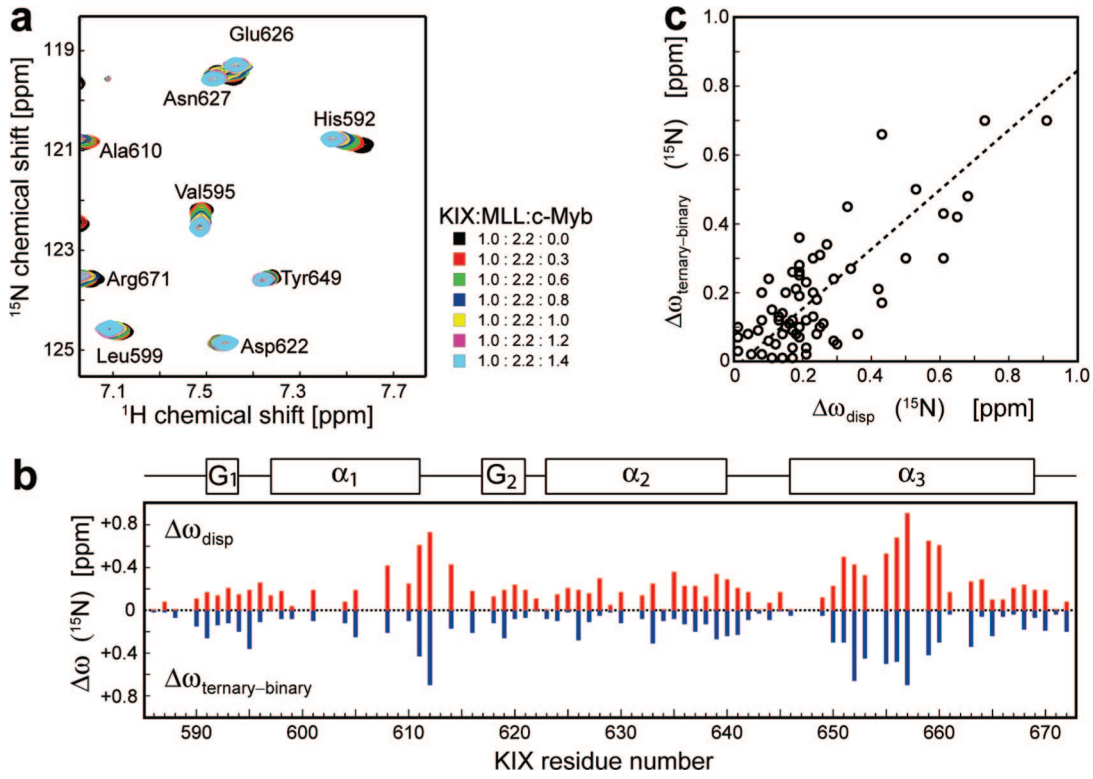

Figure 2. Chemical shift changes on c-Myb binding to the binary KIX·MLL complex. (a) [^{1}H−^{15}N]-HSQC spectra of ^{15}N-KIX bound to unlabeled MLL are shown with c-Myb concentrations ranging from 0 (black) to saturating (cyan), corresponding to KIX:MLL:c-Myb concentration ratios between 1:2.2:0 and 1:2.2:1.4. (b) Comparison of absolute values of backbone amide ^{15}N chemical shift differences obtained from relaxation dispersion data for the binary KIX·MLL complex, $\Delta\omega_{disp}$ (red bars), with absolute values of chemical shift differences between ternary KIX·MLL·c-Myb and binary KIX·MLL, $\Delta\omega_{ternary-binary}$ (blue bars). Values of $\Delta\omega_{ternary-binary}$ were determined from the titration of KIX·MLL with c-Myb and confirmed using triple-resonance NMR experiments. The location of KIX secondary structure elements in KIX·MLL·c-Myb is indicated. (c) Correlation of ^{15}N $\Delta\omega_{ternary-binary}$ and $\Delta\omega_{disp}$ values with a slope of 0.86. Because resonances are observed at population-averaged frequencies in HSQC spectra (fast exchange on the NMR chemical shift time-scale), $\Delta\omega_{ternary-binary}$ as observed upon transition from binary KIX·MLL (7% binding competent state) to fully saturated ternary KIX·MLL·c-Myb amounts to 93% of $\Delta\omega_{disp}$ values (corresponding to a slope of 0.93).

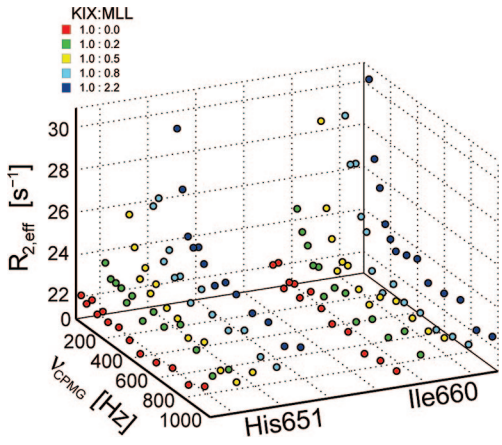

Figure 3. ^{15}N relaxation dispersion profiles for KIX at 800 MHz and 27 °C recorded at KIX:MLL concentration ratios between 1:0 and 1:2.2. Two residues distal to the MLL binding site with $\Delta\omega_{disp}$ exceeding the mean by $>2\sigma$ in the binary KIX·MLL complex are shown. For these residues $\Delta\omega_{KIX\cdot MLL-KIX}$ (due to MLL binding) < 0.2 ppm, ensuring minimal exchange contributions arising from the reversible MLL binding process under conditions where MLL is not present in excess. In addition, partial unfolding for unliganded KIX does not contribute significantly to the relaxation dispersion profiles of these residues.[49] Due to the low number of residues that fulfill these criteria we abstained from quantitative analysis of the experimental relaxation dispersion data at variable KIX:MLL concentration ratios. It is clear, however, that the higher energy state of KIX becomes progressively populated as the binary KIX·MLL complex is formed.

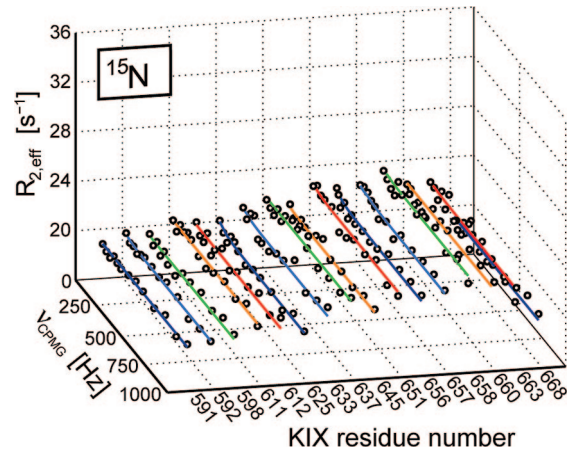

Figure 4. ^{15}N NMR relaxation dispersion profiles for representative residues of KIX bound to MLL and pKID (concentration ratio KIX:MLL:pKID = 1:2.2:1.2) recorded at 800 MHz and 27 °C. pKID was chosen as a ligand because of the ~6-fold higher affinity of KIX·MLL for pKID than for c-Myb,[21] which minimizes contributions to relaxation dispersion profiles arising from the reversible ligand binding process. Under the conditions used, >99.7% of KIX is bound to pKID.

are populated in the absence of ligand.[37] The direct experimental observation of the dynamic transition between these two

(37) Monod, J.; Wyman, J.; Changeux, J. P. *J. Mol. Biol.* **1965**, *12*, 88–118.

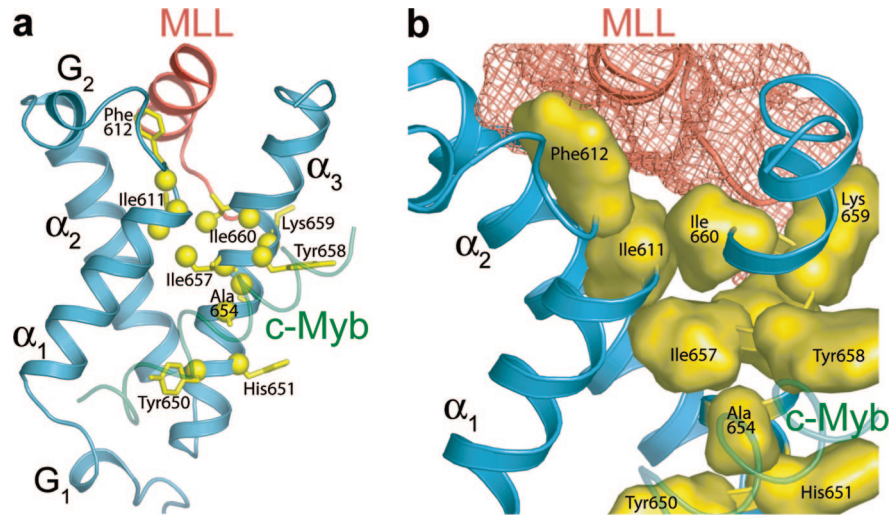

Figure 5. Allosteric network of KIX. (a) Ribbon representation of the ternary KIX·MLL·c-Myb complex (PDB entry code 2AGH).[18] The backbone of KIX (residues 586−672) is shown in blue, and elements of secondary structure are labeled. The MLL backbone (only the structured part, residues 2843−2857) is shown as red ribbon, while the backbone of c-Myb (residues 291−309), which was absent in the relaxation dispersion experiments, is shown in green (partly transparent). Yellow spheres are drawn for nuclei with $\Delta\omega_{disp}$ values exceeding the average by more than two standard deviations σ ($\Delta\omega_{disp} > 0.60$ ppm for ^{15}N, $\Delta\omega_{disp} > 0.27$ ppm for $^{13}C^{\alpha}$), and the side chains of these residues are shown. The positions of these residues largely agree with those inferred from an exhaustive compilation of chemical shift data.[18] Isoleucine side chain-δ1 carbons of Ile660, Ile611, and Ile657 are indicated by yellow spheres (see Figure 6). (b) Close-up view of the allosteric network of KIX·MLL showing the residues that bridge the MLL and c-Myb binding sites. For side chains of residues with $\Delta\omega_{disp}$ exceeding the mean by $>2\sigma$ van der Waals surfaces are drawn (yellow) and labeled, while the van der Waals surface of MLL is represented by a red wire frame. Notably, only a subset of the KIX residues that interact with MLL form part of the allosteric network.

conformers in KIX·MLL by NMR relaxation dispersion spectroscopy provides insight into the communication mechanism that links the two binding sites and mediates signal transduction: The subset of residues that display the largest chemical shift changes during this conformational transition form a tightly coupled network of interactions (Figure 5a). These residues include Tyr650, His651, Ala654, Ile657, and Tyr658. Their side chains participate in formation of a shallow hydrophobic groove on the surface of KIX, which is located between helices α_1 and α_3 and serves as docking interface for the hydrophobic face of the amphipathic helix of the c-Myb activation domain (as well as the activation domain of CREB, pKID).[18,38] Others, such as Phe612, are located distal to the c-Myb/pKID binding site, in particular at the carboxy-terminal region of helix α_1 and the short loop between helix α_1 and the 3_{10}-helix G_2. This specific region of KIX has been shown to be critical for the interaction with MLL: Upon MLL binding this loop and the 3_{10}-helix G_2 are repositioned to allow the side chain of Phe612 to make close hydrophobic contacts with the MLL amphipathic helix.[18]

Further residues that display significant chemical shift changes upon major/minor state transition and serve to bridge the two binding sites are shown in Figure 5b. Ile611, located at the carboxy terminus of helix α_1, is close to the MLL binding site and has contacts with Phe612. Its side chain does not interact with MLL but protrudes into the hydrophobic core of the KIX domain, where it interacts with Ile657 through extensive hydrophobic contacts, thereby interlinking the carboxy terminus of helix α_1 with the remote c-Myb/pKID binding surface. Likewise, Ile660 has contacts with residues in the N-terminal region of the structured part of the MLL peptide and with Ile611. To further explore the allosteric network we performed ^{13}C relaxation dispersion experiments on the side chains of isoleucine residues (δ1 methyl groups), Figure 6a. The side chain data can be fitted to the same conformational transition process as the backbone ^{15}N and $^{13}C^{\alpha}$ data with a time constant of 3 ms and a population ratio of 93:7, suggesting that the conformational rearrangements within the isoleucine cluster formed by Ile611, Ile657, and Ile660 and the protein backbone occur in a collective manner. Again, the $^{13}C^{\delta1}$ relaxation dispersion $\Delta\omega_{disp}$ values agree well with the chemical shift changes upon formation of the ternary complex with c-Myb (Figure 6b). We conclude that the side chains of these isoleucine residues participate in formation of the allosteric network and constitute the link through which allosteric information is transmitted. Sequence comparison shows that these three residues are highly conserved in KIX domains (Figure S6 in the Supporting Information) in line with the notion that functional coupling between residues in proteins represents an evolutionary constraint.[39,40]

Cooperativity has also been reported for binding of MLL to KIX in complex with c-Myb or pKID.[21] To study allosteric communication in this direction we performed relaxation dispersion experiments on a binary complex where the c-Myb/pKID binding site was occupied by ligand (Figure S7 in the Supporting Information). Flat dispersion profiles were obtained so that the communication process cannot be monitored by this technique either because the population of any higher energy state(s) that might be present is too low and/or the time scale of the process is outside the micro- to millisecond window. This finding is in line with predictions from computer simulations, which show that allosteric communication pathways are not necessarily bidirectional.[41,42]

Transcription factors stimulate gene transcription by binding to gene-specific DNA promoter sites and recruiting the basal

(38) Radhakrishnan, I.; Perez-Alvarado, G. C.; Parker, D.; Dyson, H. J.; Montminy, M. R.; Wright, P. E. *Cell* **1997**, *91*, 741–752.
(39) Süel, G. M.; Lockless, S. W.; Wall, M. A.; Ranganathan, R. *Nat. Struct. Biol.* **2003**, *10*, 59–69.
(40) Lockless, S. W.; Ranganathan, R. *Science* **1999**, *286*, 295–299.
(41) Hilser, V. J.; Dowdy, D.; Oas, T. G.; Freire, E. *Proc. Natl. Acad. Sci. U.S.A.* **1998**, *95*, 9903–9908.
(42) Chen, J.; Dima, R. I.; Thirumalai, D. *J. Mol. Biol.* **2007**, *374*, 250–266.

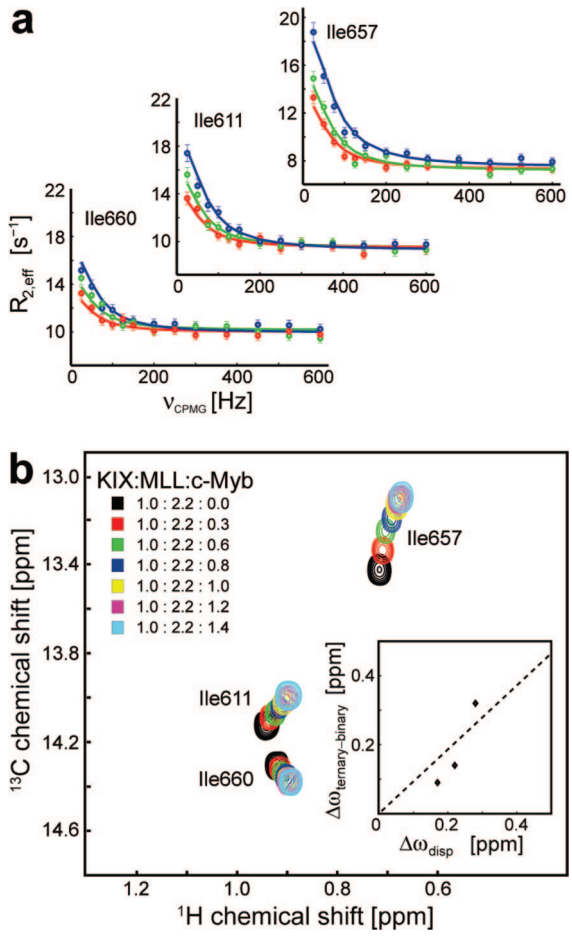

Figure 6. (a) Isoleucine $^{13}C^{\delta1}$ relaxation dispersion profiles recorded at 500 (red), 600 (green), and 800 MHz (blue) at 27 °C along with best fits. (b) Portions of [$^{1}H-^{13}C$]-HSQC spectra of KIX bound to MLL showing the positions of isoleucine side chain methyl ($\delta1$) cross peaks at c-Myb concentrations ranging from 0 (black) to saturating (cyan) corresponding to KIX:MLL:c-Myb concentration ratios between 1:2.2:0 and 1:2.2:1.4. The insert shows the correlation of absolute values of $^{13}C^{\delta1}$ $\Delta\omega_{ternary-binary}$ and $\Delta\omega_{disp}$. A dashed line with a slope of 0.93 is drawn.

transcriptional complex through their activation domains.[43] CBP plays a central role in this process because it functions as a direct link between a variety of transcription factors and components of the transcriptional machinery.[17] Because it is present at limiting concentrations in vivo, competition of different transcription factors for CBP is believed to be crucial for the regulation of gene transcription.[44] Moreover, since specificity of transcription is achieved by unique combinations of promoter-bound transcription factors, any (cooperative) effects that enhance or decrease their affinities to CBP can potentially promote specificity.[45] Our quantitative analysis of the allosteric transition in the KIX domain of CBP provides an atom-resolved description of the mechanism through which this domain mediates pairwise cooperativity between transcription factors. Binding of MLL induces a population shift of KIX conformations by ~7% toward a higher affinity conformer, which results in a ~2-fold increase of the affinities for c-Myb and pKID.[21] This population shift mechanism allows, in principle, the modulation of binding affinities in a versatile manner by the extent to which the higher affinity conformer is populated. Such pairwise fine tuning of affinities may be critical for regulation of the specificity of gene transcription, and several lines of evidence indicate that cooperative interactions between transcription factors (mediated by CBP) can promote synergism in transcriptional activation.[46,47] Moreover, the rate at which allosteric information is transmitted between binding sites might pose an essential constraint for the flow of information through the networks of proteins that regulate gene transcription in the cell.[48] Our results underline that knowledge of both structure and dynamics are required to understand the intricate molecular mechanisms by which proteins process information to fulfill their biological tasks.

Acknowledgment. We thank C. Haas and M. Ortbauer for sample preparations. This work was supported by the Austrian Science Fund (FWF), the Austrian Academy of Sciences, and the French Research Agency (ANR).

Supporting Information Available: Seven supporting figures, showing backbone hydrogen/deuterium exchange and temperature dependent data, supplementary relaxation dispersion data, a chemical shift comparison, and a sequence alignment of KIX domains, and supporting references. This material is available free of charge via the Internet at http://pubs.acs.org.

JA809947W

(43) Brivanlou, A. H.; Darnell, J. E., Jr. *Science* **2002**, *295*, 813–818.
(44) Vo, N.; Goodman, R. H. *J. Biol. Chem.* **2001**, *276*, 13505–13508.
(45) Merika, M.; Thanos, D. *Curr. Opin. Genet. Dev.* **2001**, *11*, 205–208.
(46) Carey, M. *Cell* **1998**, *92*, 5–8.
(47) Ptashne, M.; Gann, A. *Nature* **1997**, *386*, 569–577.
(48) Rousseau, F.; Schymkowitz, J. *Curr. Opin. Struct. Biol.* **2005**, *15*, 23–30.
(49) Tollinger, M.; Kloiber, K.; Agoston, B.; Dorigoni, C.; Lichtenecker, R.; Schmid, W.; Konrat, R. *Biochemistry* **2006**, *45*, 8885–8893.

Supplementary Material:

Direct Observation of the Dynamic Process Underlying Allosteric Signal Transmission

Sven Brüschweiler[†], Paul Schanda[‡], Karin Kloiber[†], Bernhard Brutscher[‡], Georg Kontaxis[†], Robert Konrat[†], and Martin Tollinger[†]*

[†] Department of Biomolecular Structural Chemistry, Max F. Perutz Laboratories, Campus Vienna Biocenter 5, A-1030 Vienna, Austria

[‡] Institut de Biologie Structurale Jean-Pierre Ebel, CNRS; CEA; UJF; 41 rue Jules Horowitz, F-38027 Grenoble, France

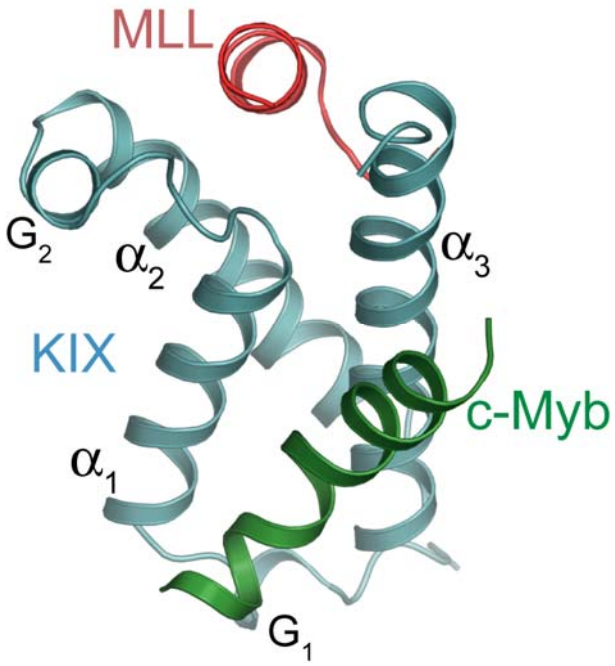

Supplementary Figure 1. Structure of the ternary KIX·MLL·c-Myb complex (PDB entry 2AGH).[1] KIX residues 586–672 are shown as light blue ribbon and elements of secondary structure are labeled. The backbone of the structured parts of the MLL (residues 2843–2857) and the c-Myb (residues 291–309) activation domains are shown as red and green ribbon, respectively.

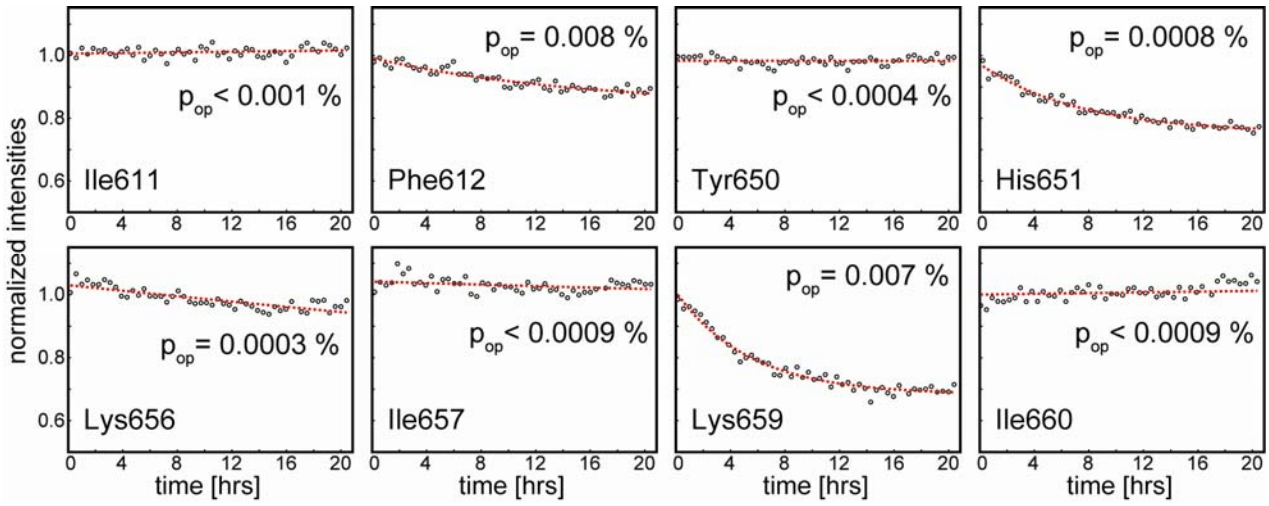

Supplementary Figure 2. Backbone amide H/D exchange data (populations of exchange-competent states, p_{op}) recorded on the binary KIX·MLL complex (concentration ratio 1:2.2) at 27°C for selected residues with $\Delta\omega_{disp}$ exceeding the mean by >2σ in the binary KIX·MLL complex. For all residues in KIX·MLL values of p_{op} are < 0.04%.

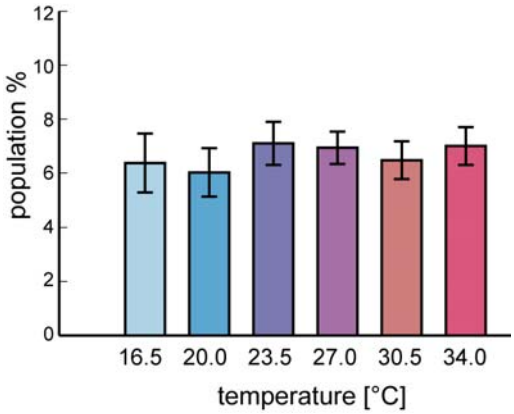

Supplementary Figure 3. Temperature dependence of the population of the higher energy state that is present in KIX·MLL, obtained from ^{15}N NMR relaxation dispersion experiments recorded at 16.5, 20.0, 23.5, 27.0, 30.5 and 34.0°C.

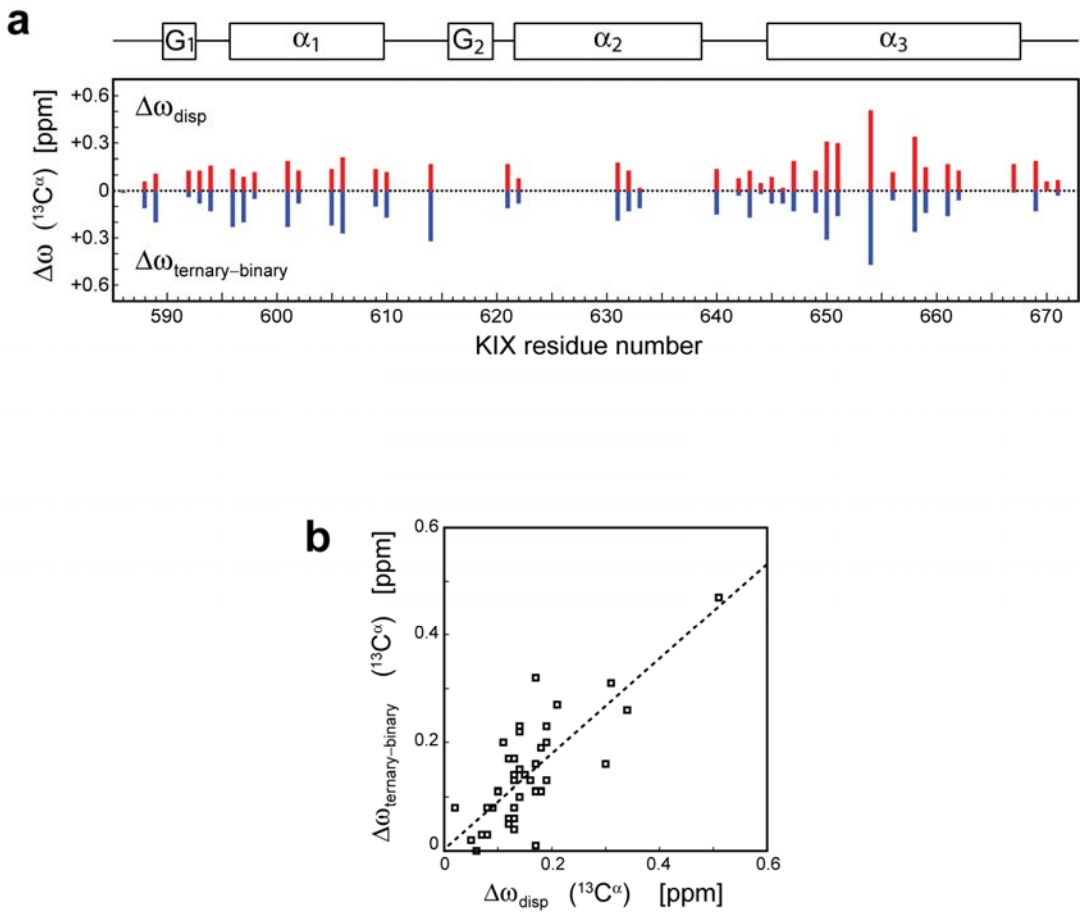

Supplementary Figure 4. KIX $^{13}C^{\alpha}$ chemical shift changes upon binding c-Myb to the KIX·MLL complex. (**a**) Comparison of absolute values of $^{13}C^{\alpha}$ chemical shift differences obtained from relaxation dispersion data for the binary KIX·MLL complex, $\Delta\omega_{disp}$, (red bars) with absolute values of $^{13}C^{\alpha}$ chemical shift differences between the ternary KIX·MLL·c-Myb complex and the binary KIX·MLL complex, $\Delta\omega_{ternary-binary}$, (blue bars). Values of $\Delta\omega_{ternary-binary}$ were determined using triple-resonance NMR experiments (HNCA and HN(CO)CA). The location of KIX secondary structure elements in the ternary KIX·MLL·c-Myb complex is indicated. (**b**) Correlation of $^{13}C^{\alpha}$ $\Delta\omega_{ternary-binary}$ and $\Delta\omega_{disp}$ values. The linear correlation coefficient is 0.78, the slope is 0.89.

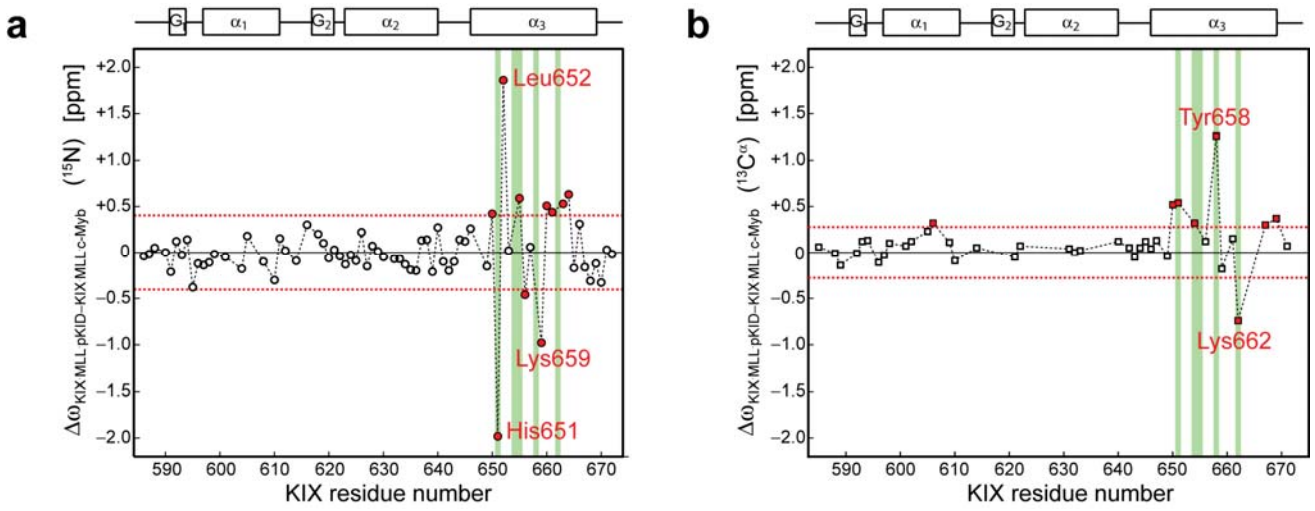

Supplementary Figure 5. Comparison of chemical shifts in the two ternary complexes KIX·MLL·c-Myb and KIX·MLL·pKID. Differences of backbone amide ^{15}N (**a**) and $^{13}C^{\alpha}$ (**b**) chemical shift values between the ternary complexes, $\Delta\omega_{KIX\cdot MLL\cdot pKID–KIX\cdot MLL\cdot c\text{-}Myb}$, are plotted as a function of KIX residue number. Red dashed lines are drawn at ±σ, where σ is the standard deviation of all $\Delta\omega_{KIX\cdot MLL\cdot pKID–KIX\cdot MLL\cdot c\text{-}Myb}$ values (σ (^{15}N)=0.40, σ ($^{13}C^{\alpha}$)=0.28). Residues with values of $\Delta\omega_{KIX\cdot MLL\cdot pKID–KIX\cdot MLL\cdot c\text{-}Myb}$ exceeding σ are indicated in red. KIX residues Tyr658 and Lys662, which specifically interact with the charged phosphate group of the phosphoserine 133 of pKID (the equivalent residue is Arg294 in c-Myb), as well as KIX residues Tyr651, Ala654, Glu655 and Tyr658, which interact with the aromatic side chain of Tyr134 of pKID (the equivalent residue in c-Myb is Ile297, and c-Myb does not contain any aromatic amino acids) are highlighted in light green. $\Delta\omega_{KIX\cdot MLL\cdot pKID–KIX\cdot MLL\cdot c\text{-}Myb}$ values are only shown for residues for which relaxation dispersion data were obtained.

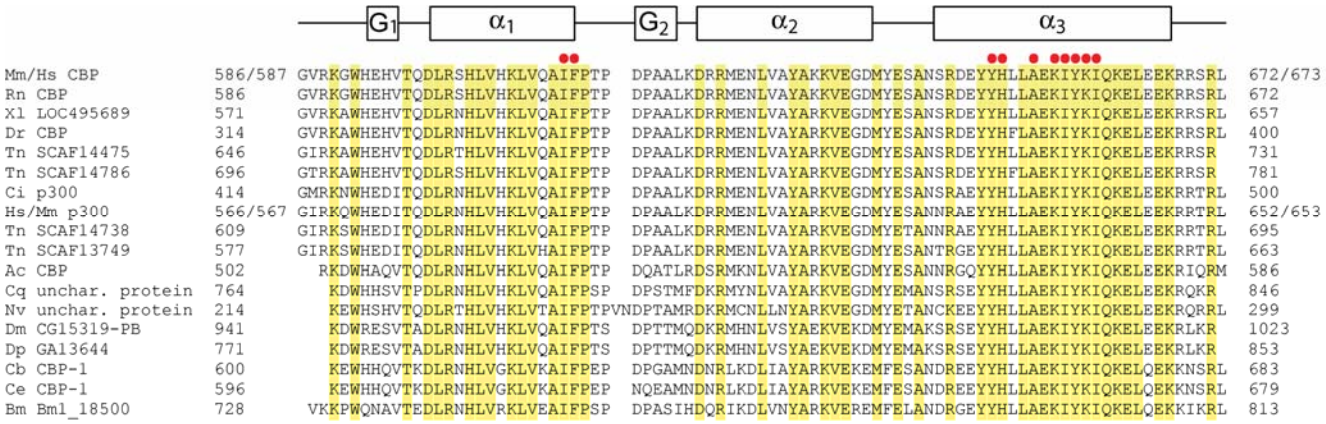

Supplementary Figure 6. Alignment of KIX domain sequences from various species (prefix abbreviations; Mm, *Mus musculus*; Hs, *Homo sapiens*; Rn, *Rattus norvegicus*; Xl, *Xaenopus laevis*; Dr, *Danio rerio*; Tn, *Tetraodon nigroviridis*; Ci, *Ctenopharyn-godon idella*; Ac, *Aplysia californica*; Cq, *Culex quinquefasciatus*; Nv, *Nemato-stella vectensis*; Dm, *Drosophila melanogaster*; Dp, *Drosophila pseudoobscura*; Cb, *Caenorhabditis briggsae*; Ce, *Caenorhabditis elegans*; Bm, *Brugia malayi*). Residues that are invariant in these proteins are highlighted in yellow, and residues that participate in the allosteric network of the binary KIX·MLL complex ($\Delta\omega_{disp}$ values exceed the average by >2σ for ^{15}N and/or $^{13}C^{\alpha}$) are indicated by red dots. The location of KIX secondary structure elements is shown.

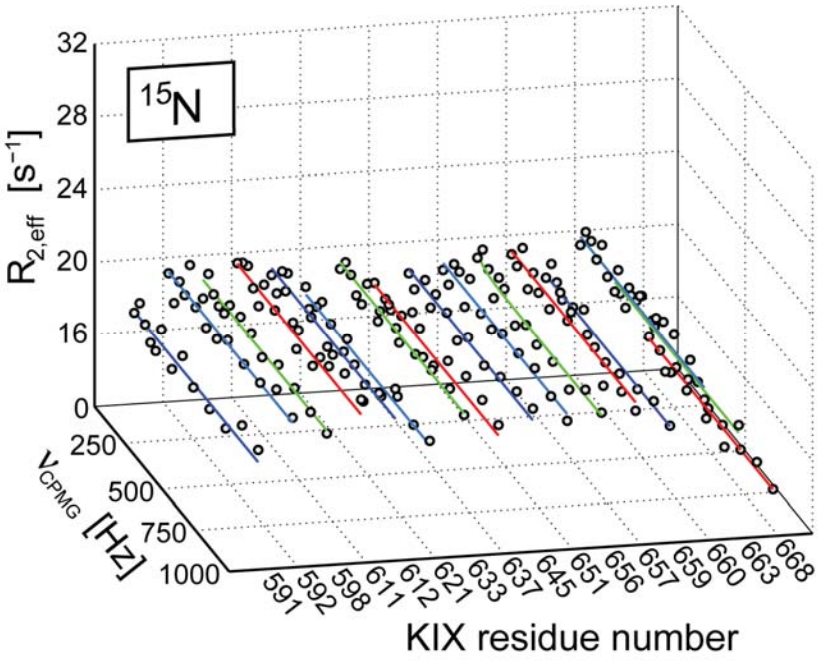

Supplementary Figure 7. NMR ^{15}N relaxation dispersion profiles of representative residues in the binary KIX·pKID complex (concentration ratio KIX: pKID=1:1.2, higher concentrations of pKID were avoided to prevent binding of pKID to the MLL binding site,[2] recorded at 600 MHz and 27°C. pKID was chosen as a ligand for the c-Myb/pKID binding site because of the ~8-fold higher affinity of KIX for pKID than for c-Myb.[3] Under the conditions used, >99.6% of KIX is bound to pKID.

References.

1. De Guzman, R.N., Goto, N.K., Dyson, H.J. & Wright, P.E. Structural basis for cooperative transcription factor binding to the CBP coactivator. *J Mol Biol* **355**, 1005–1013 (2006).
2. Sugase, K., Dyson, H.J. & Wright, P.E. Mechanism of coupled folding and binding of an intrinsically disordered protein. *Nature* **447**, 1021–1025 (2007).
3. Goto, N.K., Zor, T., Martinez-Yamout, M., Dyson, H.J. & Wright, P.E. Cooperativity in transcription factor binding to the coactivator CREB-binding protein (CBP). *J Biol Chem* **277**, 43168–43174 (2002).